High spin states in ^{162}Lu

S. L. Gupta,[1] S. C. Pancholi,[1] P. Juneja,[1] D. Mehta,[1] Ashok Kumar,[1] R. K. Bhowmik,[2] S. Muralithar,[2] G. Rodrigues,[2] and R. P. Singh[2]

[1]*Department of Physics and Astrophysics, University of Delhi, Delhi-110007, India*

[2]*Nuclear Science Centre, Aruna Asaf Ali Marg, New Delhi-110067, India*

(Received 30 January 1997)

An experimental investigation of the odd-odd ^{162}Lu nucleus, following the ^{148}Sm(^{19}F,5n) reaction at beam energy $E_{\rm lab}$=112 MeV, has been performed through in-beam gamma-ray spectroscopy. It revealed three signature-split bands. The yrast band based on $\pi h_{11/2}\otimes \nu i_{13/2}$ configuration exhibits anomalous signature splitting (the unfavored signature Routhian lying lower than the favored one) whose magnitude $\Delta e' \approx 25$ keV, is considerably reduced in contrast to sizable normal signature splitting $\Delta e' \approx 125$ and 60 keV observed in the yrast $\pi h_{11/2}$ bands of the neighboring odd-A ^{161,163}Lu nuclei, respectively. The signature inversion in this band occurs at spin $\sim 20\hbar$ (frequency=0.37 MeV). The second signature-split band, observed above the band crossing associated with the alignment of a pair of $i_{13/2}$ quasineutrons, is a band based on the four-quasiparticle $[\pi h_{11/2}[523]7/2^- \otimes \nu h_{9/2}[521]3/2^- \otimes (\nu i_{13/2})^2]$, i.e., $EABA_p(B_p)$, configuration. The third signature-split band is also likely to be a four-quasiparticle band with configuration similar to the second band but involving F quasineutron, i.e., $FABA_p(B_p)$. The experimental results are discussed in comparison with the existing data in the neighboring nuclei and in the framework of the cranking shell model. [S0556-2813(97)01809-8]

PACS number(s): 21.10.Re, 23.20.Lv, 23.20.En, 27.70.+q

I. INTRODUCTION

The study of high spin states in deformed odd-odd nuclei in the rare-earth region has received added attention during the recent past, resulting in the observation of a number of interesting phenomena. One of the most striking features has been the anomalous signature splitting observed in the high-K $\pi h_{11/2}\otimes \nu i_{13/2}$ yrast band in ^{152}Eu [1], $^{154-156}$Tb [2], $^{156-162}$Ho [3–8], $^{158-164}$Tm [9–14], ^{160,164,166}Lu [15–18], and ^{168}Ta [19] nuclei. In this band, the unfavored ($\alpha=1$) signature lies lower than the favored ($\alpha=0$) one, a behavior opposite to what is expected from the $\pi h_{11/2}$ yrast band in the neighboring odd-Z nuclei [20–24]. The experimental Routhians for the two signatures cross each other (signature inversion) at a rotational frequency characteristic of the nucleus, thereby restoring normal signature splitting. Attempts have been made to interpret signature inversion in these odd-odd nuclei using several models such as the cranking shell model [25,26], the particle rotor model [27–29], the angular-momentum-projection method [30,31], and the interacting boson-fermion model [32]. Another interesting feature noticed is the disappearance of the odd neutron blocking effect in the $\pi g_{7/2}\otimes \nu h_{9/2}$ band in odd-odd ^{158}Ho [6] and the $\pi h_{11/2}\otimes \nu h_{9/2}$ band in ^{160,162}Tm [10,11] and ^{164}Lu nuclei [16,17]. The AB band crossing being observed in these bands is at $\sim$0.28 MeV, which is close to that observed in neighboring even-even nuclei [33]. However, in the $\nu h_{9/2}$ band of the neighboring odd-N, even-Z nuclei [33], the AB neutron band crossing occurs at a lower rotational frequency ($\hbar\omega \sim 0.23$ MeV) due to the blocking effect of the odd neutron causing a reduction of the neutron pair correlations. The abnormally large AB neutron band crossing frequencies may be related to the neutron-proton residual interactions in these odd-odd nuclei. Further, such a band crossing anomaly is not observed in the $\pi h_{11/2}\otimes \nu h_{9/2}$ band in odd-odd ^{164}Tm [13]. Therefore, more experimental investigations in odd-odd nuclei are needed to understand this effect. Another feature which has come to light is the population of a signature-split four-quasiparticle $[\pi h_{11/2}\otimes \nu h_{9/2}\otimes (\nu i_{13/2})^2]$ band in odd-odd ^{158}Tm [9] and ^{164}Lu [17], observed only above the AB neutron band crossing.

In this paper, the results on the high spin states in odd-odd ^{162}Lu nucleus are presented. This work revealed three signature-split bands. In the yrast band based on the $\pi h_{11/2}\otimes \nu i_{13/2}$ configuration, anomalous signature splitting has been observed with signature inversion occuring at $I\sim 20\hbar$. The other two bands are probably the four-quasiparticle band structures observed above the AB neutron band crossing, similar to the one seen in ^{158}Tm [9]. The present work is the first investigation of high spin states in ^{162}Lu. Preliminary reports on our work on this nucleus were presented earlier [34]. Very recently, short communications [35–37] reporting the yrast sequence in this nucleus have also appeared in the literature. Results reported therein are in general agreement with the present work.

II. EXPERIMENTAL DETAILS AND ANALYSIS

The search for high spin states belonging to ^{162}Lu was performed through the ^{148}Sm(^{19}F,5n)^{162}Lu fusion-evaporation reaction at a beam energy of 112 MeV. The target used was an enriched ^{148}Sm self-supporting foil of thickness $\sim 850\ \mu$g/cm^2. The ^{19}F ion beam was provided by the 15 MV pelletron accelerator at the Nuclear Science Centre (NSC), New Delhi. The beam energy was selected by performing PACE calculations [38] and by generating experimental excitation functions at different beam energies in the range 108–120 MeV. PACE calculations [38] predict that the population curve corresponding to the $p4n$(^{162}Yb) channel lies right below that of the $5n$(^{162}Lu) channel. Prior to this work, the only available information about ^{162}Lu was regard-

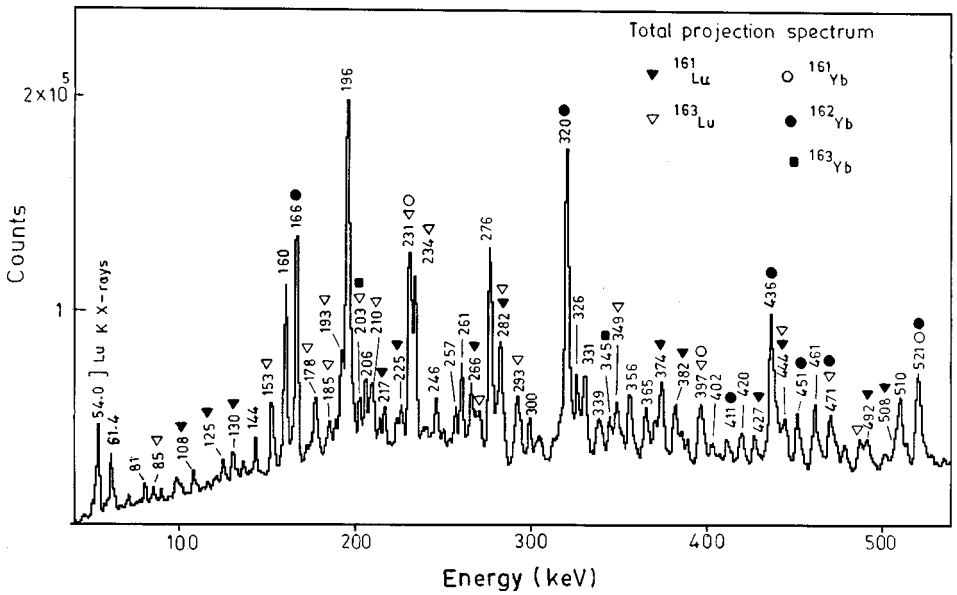

FIG. 1. Total projection spectrum generated from the E_γ-E_γ coincidence matrix from the ^{148}Sm(^{19}F,5n) reaction at an incident beam energy of 112 MeV.

ing the gamma lines at 174, 196, and 410 keV observed in the radioactive decay of ^{162}Hf [39,40]. A beam energy of 112 MeV was found to be optimum, at which the observed yields of both the $4n$(^{163}Lu) and $6n$(^{161}Lu) reaction channels were minimum relative to the $p4n$(^{162}Yb) channel. At this beam energy, reaction products identified were ^{161}Lu (11%), ^{161}Yb (8%), ^{162}Lu (36%), ^{162}Yb (23%), ^{163}Yb (3%), and ^{163}Lu (15%) (Fig. 1).

Gamma rays emitted by the evaporation residues were detected using the Gamma Detector Array (GDA) [41]. The array consisted of 6 Compton-suppressed Ge detectors and a 14-element bismuth germanate (BGO) multiplicity filter. The Ge detectors, located at 18 cm from the target position, were mounted in two groups of three each, making angles of 99° and 153° with the beam direction and having an inclination of $\pm 22.5°$ with the horizontal plane. The multiplicity filter consisted of two groups of seven hexagonal BGO elements (3.8 cm$\times$7.5 cm long), each mounted above and below the target chamber at a distance of 4 cm from the target. A total of 100×10^6 $\gamma\gamma$-coincidence events were collected during the experiment. The detector efficiencies and energy calibration of Ge detectors were deduced from singles spectra measured using the ^{133}Ba and ^{152}Eu radioactive sources. After gain matching to 0.5 keV/channel and correcting for the Doppler shift, the coincidence data were sorted into $4k\times4k$ E_γ-E_γ matrix with the requirement of more than one BGO multiplicity detector firing. The gamma-ray coincidence relationships were established by setting gates on the photopeaks of individual transitions assigned to the ^{162}Lu nucleus and projecting the coincident spectra. Gates were also set on the background in the vicinity of the photopeaks to remove the contributions due to the coincident background underlying the photopeaks of the gated transitions.

Since no high spin level scheme of ^{162}Lu has been reported previously, gamma transitions belonging to this nucleus have been identified by following the usual x-ray/gamma-ray gating and the reaction channel elimination procedures: A coincidence spectrum with the gate on Lu K x rays showed a large number of γ lines, as shown in Fig. 2. After identifying the previously known γ rays in ^{161}Lu [20] and ^{163}Lu [21] isotopes, the remaining γ rays were tentatively assigned to ^{162}Lu. Further, most of the intense γ rays like 81, 144, 160, 196, 246, 257, 261, 276 keV, etc. (as also seen in Fig. 2), observed in total projection spectrum (Fig. 1), do not belong to the other populated and previously studied ^{161,163}Lu [20,21] and $^{161-163}$Yb [42–44] nuclei and hence are assigned to ^{162}Lu. Assignment of all the other gamma transitions to ^{162}Lu is based on the coincidence relationships with these strong gamma transitions.

The level scheme of ^{162}Lu deduced from present work is shown in Fig. 3. It shows three signature-split bands (labeled band A, band B, and band C), each consisting of two strongly coupled decay sequences. A sequence of 420-535-621-643 keV $E2$ transitions, not shown in Fig. 3, has been assigned to ^{162}Lu on the basis of its coincidence relationships with the transitions of band C below spin $(X+4)$ [Figs. 4(e) and 4(f)]. Also, about 20% of the intensity of band B feeds into band A below spin 16 via a likely gamma-ray transition of 600 keV. However, a complete linking pattern could not be established in both cases. The ordering of transitions in various bands is based on $\gamma\gamma$-coincidence relationships, γ-ray energy sums, and γ-ray intensities. Gamma-ray intensities for the transitions assigned to ^{162}Lu were determined from total projection spectrum and gated coincidence spectra. The gamma-ray energies, intensities, and their placements in the level scheme are presented in Table I. In Figs. 4(a)–4(f), summed gated coincidence spectra for bands A, B, and C are displayed, which clearly show the γ lines belonging to these bands. The estimated populations for bands A, B, and C are about 56%, 28%, and 12%, respectively. It may be mentioned that bands A and B are found to be even stronger compared to the known yrast bands in the neighboring ^{161,163}Lu nuclei [20,21].

The multipolarities to the gamma transitions were assigned on the basis of measured DCO (directional correlation of γ-rays deexciting oriented states) ratios $[=I_\gamma(153°)/I_\gamma(99°)]$ [45] extracted from the coincidence data. The coincidence events were sorted into an asymmetric matrix with 153° detectors on one axis and 99° detectors on the other axis. Two different $\gamma\gamma$-correlation intensities were determined: $I_\gamma(153°)$, the γ-ray intensity measured in 153° detector while gating on a quadrupole transition de-

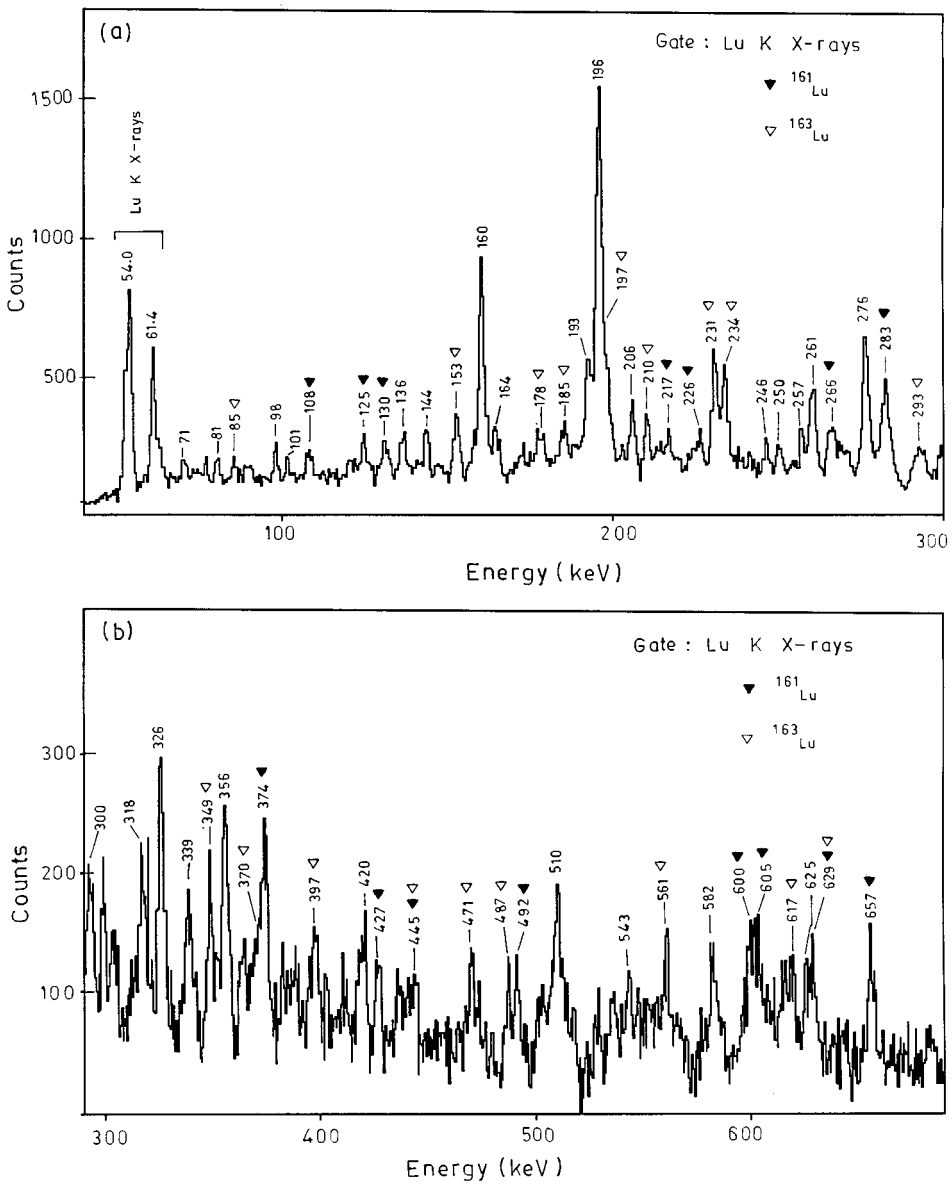

FIG. 2. Gamma-ray coincidence spectrum obtained by gating on Lu K x-rays.

tected in a 99° detector, and $I_\gamma(99°)$, from the inverse gating. For all three bands A, B, and C, low-lying crossover transitions were assumed to be stretched quadrupole ones. The extracted DCO ratios are also given in Table I. For the determination of DCO ratios of weak transitions, as many gated spectra as possible were summed in order to increase the statistics. The tabulated DCO ratios confirm the assigned dipole ($\Delta I=1$) or quadrupole ($\Delta I=2$) character of the transitions, but the experimental uncertainties are rather large due to low intensities of the transitions and the complicated nature of the spectra due to unresolved doublets and many transition energies in ^{162}Lu being close to those present in ^{161}Lu and ^{163}Lu. The character of some of the low energy dipole transitions was further confirmed to be $M1$ through intensity balance procedure.

The experimental ratios of reduced transition probabilities, $B(M1,I\rightarrow I-1)/B(E2,I\rightarrow I-2)$ in units of $(\mu_N/e\ \mathrm{b})^2$, for bands A, B, and C are deduced from the relation

$$\frac{B(M1,I\rightarrow I-1)}{B(E2,I\rightarrow I-2)}=0.697\,\frac{E_\gamma^5(I\rightarrow I-2)}{E_\gamma^3(I\rightarrow I-1)}\,\frac{1}{\lambda(1+\delta^2)}, \quad (1)$$

where E_γ is the energy of the γ ray in MeV, $\lambda=I_\gamma(I\rightarrow I-2)/I_\gamma(I\rightarrow I-1)$ is the intensity branching ratio for the level with spin I, and δ is the $E2/M1$ mixing ratio for the $\Delta I=1$ transition. In our calculations, we assumed $\delta^2=0$. This assumption does not influence the experimental results since the mixing ratios are generally small and the errors introduced in the $B(M1)/B(E2)$ ratios due to this assumption are rather negligible when compared to the uncertainties associated with branching ratios. The branching ratios (λ) and the $B(M1)/B(E2)$ ratios deduced from the present work for the coupled bands A, B, and C are listed in the last two columns in Table I. The $B(M1)/B(E2)$ values are also shown as a function of initial level spin in Fig. 5.

The experimental $B(M1)/B(E2)$ values are compared with the theoretical values estimated from the geometric model of Dönau and Frauendorf [46] (see also Refs. [18,23])

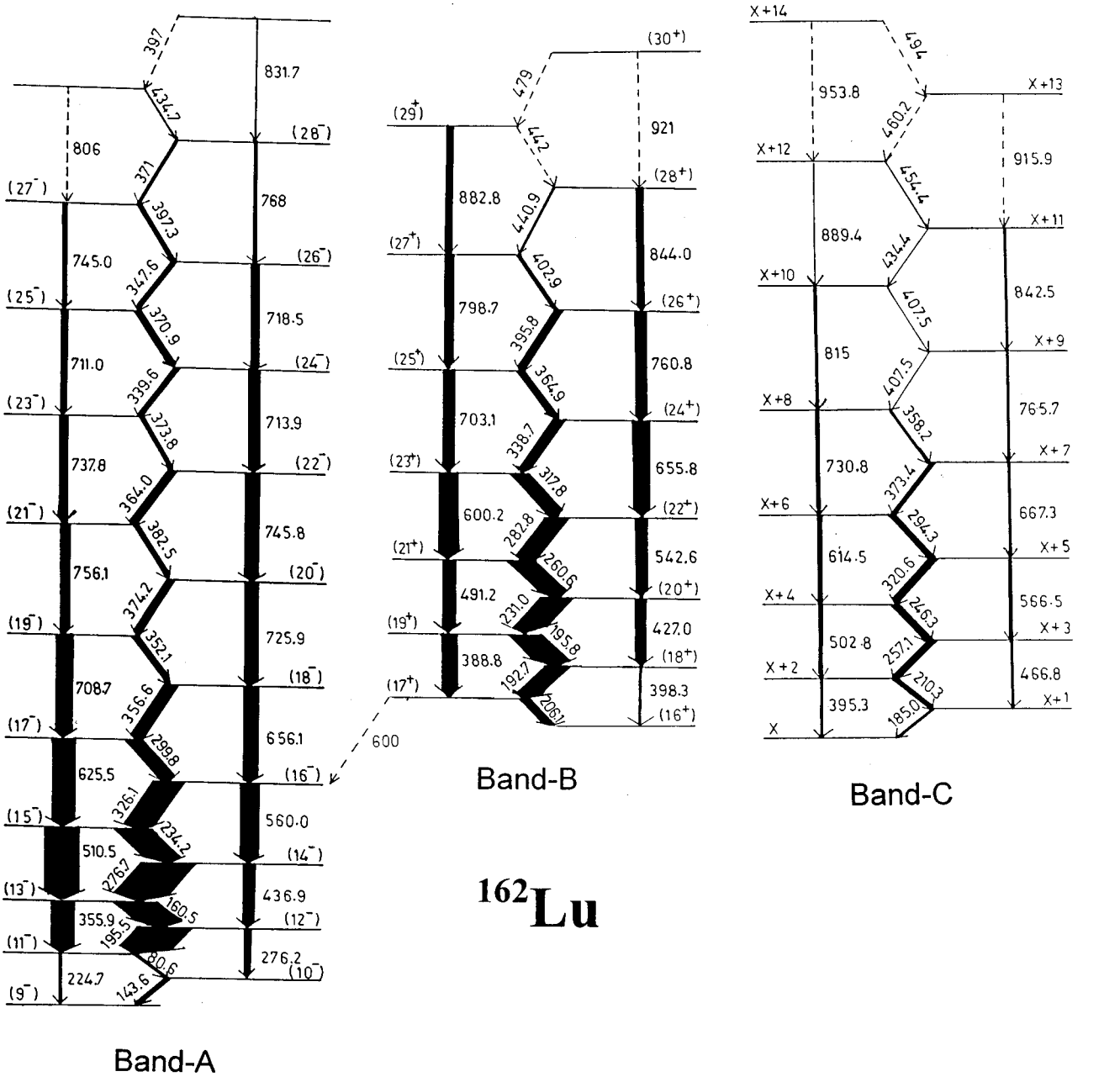

FIG. 3. Level scheme of ^{162}Lu established from the present work. The spins to levels in band *C* are relative to spin *X* assigned to the lowest shown level.

based on a cranking approach. In this model, the reduced transition probability, $B(M1)$ in units of μ_N^2, is given by

$$B(M1,I\rightarrow I-1)=|\langle II|\mu(M1)|I-1I-1\rangle|^2=\frac{3\mu_\perp^2}{8\pi}, \tag{2}$$

where $\mu_\perp$ is the component of the magnetic dipole moment perpendicular to the total spin I of the nucleus. For a rotational band in a doubly odd nucleus (before a band crossing), $\mu_\perp$ can be expressed as sum of the contributions from various participating quasiparticles, $\mu_{\perp p(n)}$'s,

$$\mu_{\perp p(n)}=(g_{p(n)}-g_R)\left[\Omega_{p(n)}\left(1-\frac{K^2}{I^2}\right)^{1/2}(1\pm S)-i_{p(n)}\frac{K}{I}\right], \tag{3}$$

where $g_{p(n)}$, $i_{p(n)}$, and $\Omega_{p(n)}$ refer to the intrinsic g factor, alignment, and the projection angular momentum component on the symmetry axis for the deformation aligned quasiproton (quasineutron), respectively. g_R is the g factor of the collective rotation. $S=\Delta e'/\hbar\omega$, corresponding to the signature-active quasiparticle, i.e., the one which is assumed to contribute both signature partners to the band, and $S=0$ otherwise. As $\Delta e'$ is small for the bands observed in ^{162}Lu, this term is not included in the above equation. In the case of $B(M1)/B(E2)$ calculations after a band crossing,

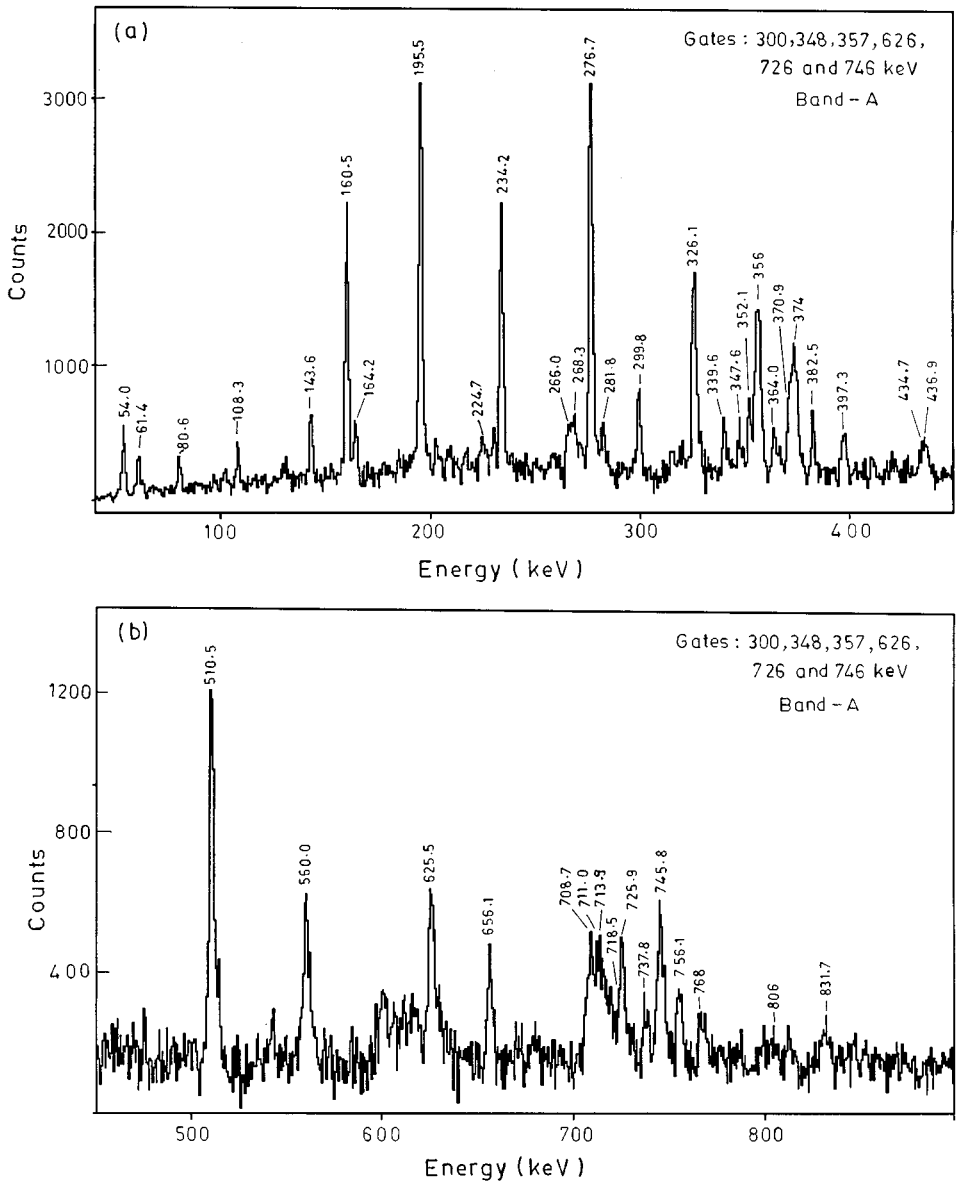

FIG. 4. Gamma-ray coincidence spectra corresponding to the sum of coincidence spectra obtained by gating different transitions (as indicated in the figures) in the bands *A*, *B*, and *C*. The peaks labeled (▼) in (e) and (f) are seen consistently in the gated coincidence spectra of transitions of band *C*. The peaks labeled (●) are contaminants.

additional terms corresponding to the rotation-aligned pairs of quasiparticles have been included in the sum.

The rotor estimate for the reduced transition probability, $B(E2,I\rightarrow I-2)$ in units of e^2 b^2, is given by

$$B(E2,I\rightarrow I-2)=\frac{5}{16\pi}\langle IK20|I-2K\rangle^2 Q_0^2, \qquad (4)$$

where Q_0 is the intrinsic quadrupole moment.

III. RESULTS AND DISCUSSION

The ^{162}Lu studied through β^+ and electron capture decay of ^{162}Hf ($T_{1/2}=37.6$ s) [39,40] was earlier known with the existence of only few low-lying states with no spin-parity information. However, Behrens [47,39] suggested $I^\pi=(1^-)$ for the ground state ($T_{1/2}=1.37$ m) of ^{162}Lu from the decay of ^{162}Lu to ^{162}Yb. Also, from this work, two isomeric states with $T_{1/2}=1.5$ and 1.9 m were proposed in ^{162}Lu.

The relative placement of bands *A*, *B*, and *C* in ^{162}Lu (Fig. 3), as observed in the present work, is arbitrary. Neither interband transitions nor transitions from these bands to the ground state could be found. The assignment of the proton and the neutron Nilsson configurations to bands *A*, *B*, and *C* is based on the experimentally deduced $B(M1)/B(E2)$ ratios, the band-crossing frequencies, and on the principle of coupling of alignments of the quasiproton and quasineutron bands in the neighboring odd-*A* nuclei. A systematic discussion of different bands observed in ^{162}Lu is given below.

A. Band *A*

Band *A* (Fig. 3), being the most intensely populated in the heavy-ion reaction used, is most likely the yrast one and has

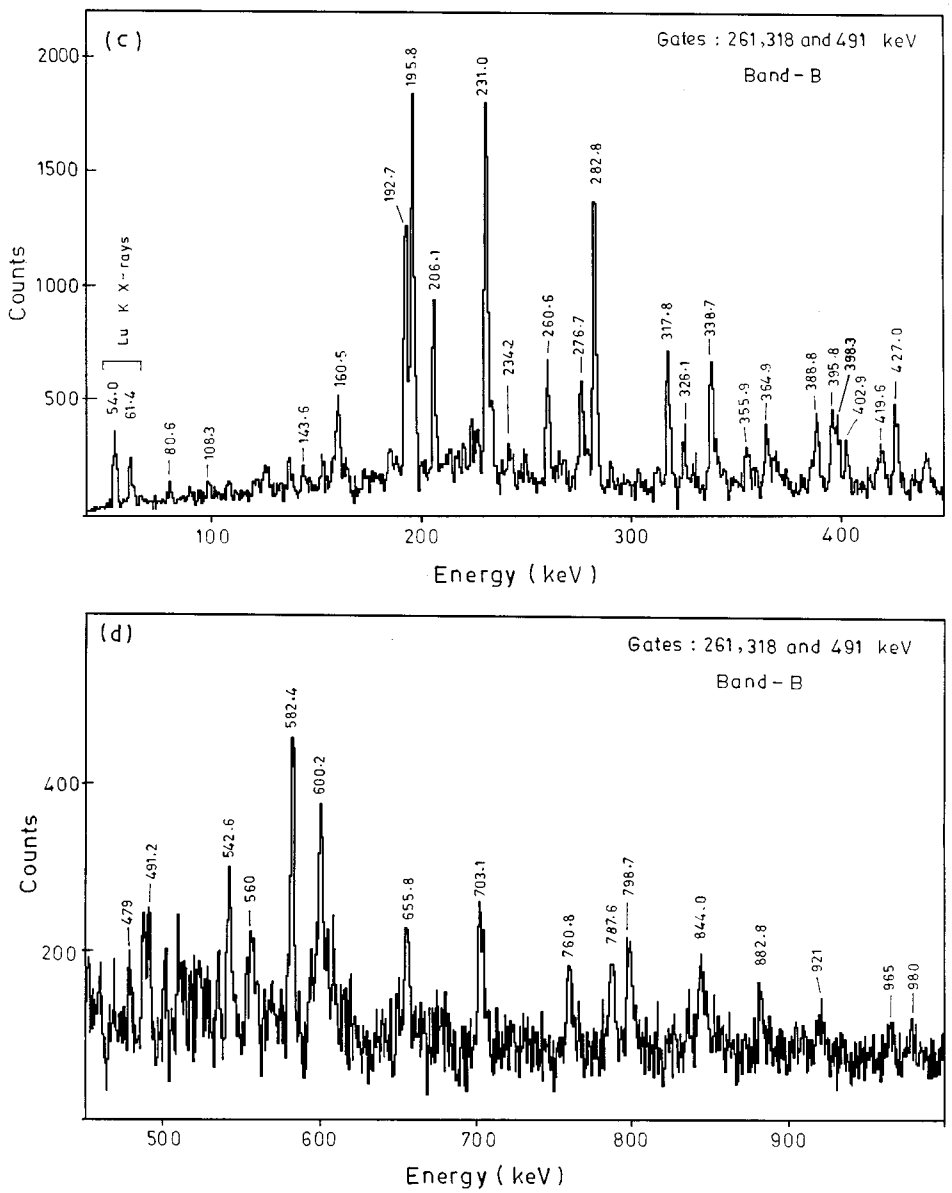

FIG. 4. (*Continued*).

been assigned a $\pi h_{11/2}[523]7/2^- \otimes \nu i_{13/2}[651]3/2^+$ Nilsson configuration. This band ends at the lower part in several parallel transitions, viz., 108, 161, 164, 266, 268, and 282 keV (not shown in Fig. 3; see Table I), which may possibly populate an isomeric state either directly or via low energy highly internally converted transitions.

In Fig. 6, the level energies vs spin of $\pi h_{11/2} \otimes \nu i_{13/2}$ yrast bands in the neighboring odd-odd $^{156-162}$Ho [3–8,48], $^{158-166}$Tm [9–14], and ^{160,164,166}Lu [15–18,48] nuclei are plotted. As is clear from this figure, the level energies of these bands exhibit smooth trends for a set of isotopes. The level energies of the yrast band (band *A*) in ^{162}Lu fit well into the systematics, favoring the $\pi h_{11/2} \otimes \nu i_{13/2}$ configuration to this band. The level spins obtained from this comparison are shown in Fig. 3.

In order to identify the possible Nilsson configuration for the yrast band in the odd-odd ^{162}Lu nucleus, we make use of the configuration of the participating proton and neutron in the yrast bands of the neighboring odd-*Z* Lu and odd-*N* Yb nuclei. The signature-split yrast bands in the neighboring odd-*Z* ^{163}Lu and ^{161,165}Lu nuclei have been assigned $\pi h_{11/2}[523]7/2^-$ [49] and $\pi h_{11/2}[514]9/2^-$ [20,22] configurations, respectively. The yrast bands in the neighboring odd-*N* ^{161}Yb and ^{163}Yb nuclei have been assigned $\nu i_{13/2}[651]3/2^+$ [42] and $\nu i_{13/2}[642]5/2^+$ [44] configurations, respectively. On this basis, the most likely Nilsson configuration for band *A* in ^{162}Lu is $\pi h_{11/2}[523]7/2^-$ (or $\pi h_{11/2}[514]9/2^-) \otimes \nu i_{13/2}[642]5/2^+$ (or $\nu i_{13/2}[651]3/2^+$). The alignment plot for band *A* (Fig. 7) gives an alignment value $i_{\text{expt}}=8.1\hbar$ for the two signatures at $\hbar\omega=0.20$ MeV. In Table II, the alignment values i_p and i_n at $\hbar\omega=0.20$ MeV before the band crossing for different band configurations in the neighboring odd-*A* nuclei and odd-odd ^{162}Lu are listed. As is clear from this table (also see Fig. 7), the additivity of the aligned angular momenta of the odd neutron and odd proton does favor the above-mentioned configurations, but obviously not uniquely.

The experimental Routhians for the two signature partners of band *A* in ^{162}Lu are plotted in Fig. 8(b) and indicate a

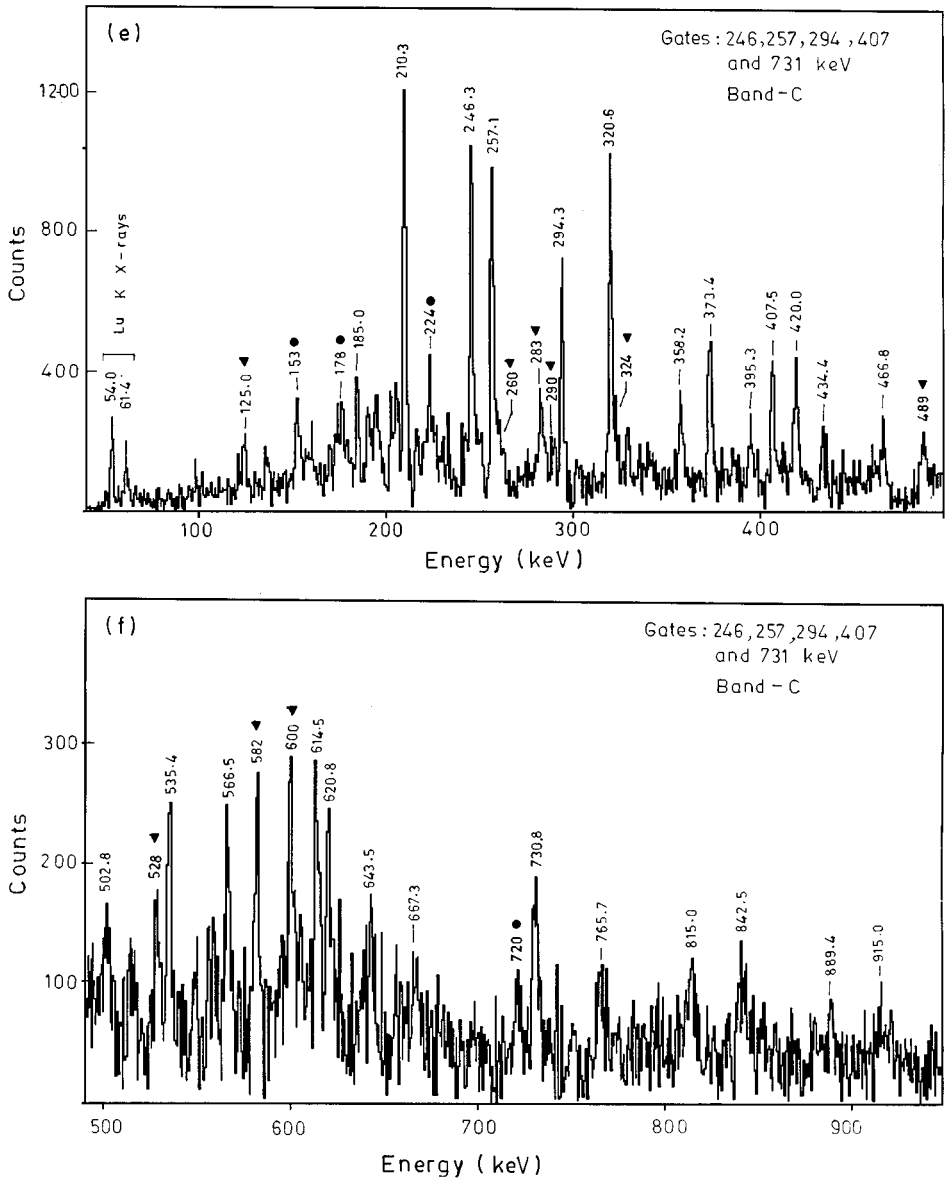

FIG. 4. (*Continued*).

band crossing at $\hbar\omega = 0.35$ MeV. This is also clear from the alignment plot (Fig. 7) in which both the signature partners show sharp upbend at about the same rotational frequency and an alignment gain $\sim 7\hbar$. This crossing frequency matches well with the value $\hbar\omega_c \approx 0.35$ MeV observed for the $i_{13/2}$ neutron BC crossing in the yrast bands in the neighboring odd-A isotopes of $_{70}$Yb, and $_{72}$Hf, and odd-odd ^{162}Tm [10–12] and ^{164,166}Lu [16–18] nuclei (see Table III). The absence of the AB neutron band crossing implies that the neutron partner in the configuration of band A is the $i_{13/2}$ neutron.

The $B(M1)/B(E2)$ ratios for this band in the region before band crossing have been calculated for the expected $\pi h_{11/2}[523]7/2^-$ (or $\pi h_{11/2}[514]9/2^-) \otimes \nu i_{13/2}[642]5/2^+$ (or $\nu i_{13/2}[651]3/2^+$) configurations using Eqs. (2)–(4) (Sec. II). The calculated values have been plotted in Fig. 5(a) and compared with the experimental ones. The parameters used for theoretical calculations are $g_n = -0.22$ [52], $i_n = 5.7\hbar$ for $\nu i_{13/2}[651]3/2^+$, $g_n = -0.25$ [12], $i_n = 5.4\hbar$ for $\nu i_{13/2}[642]5/2^+$, $g_p = 1.32$ [21], $i_p = 2.4\hbar$ for $\pi h_{11/2}[514]9/2^-$, and $g_p = 1.41$ [53], $i_p = 2.8\hbar$ for $\pi h_{11/2}[523]7/2^-$, $g_R = 0.4$ [54], $K = \Omega_p + \Omega_n$ following the Gallagher-Moszkowski rule [55], and a constant quadrupole moment of 5.1 e b [56]. As is clear from Fig. 5(a), the experimental ratios before band crossing are closer to those calculated for the configuration $\pi h_{11/2}[523]7/2^- \otimes \nu i_{13/2}[651]3/2^+$. Also, keeping in mind the yrast configurations in odd-Z ^{163}Lu and odd-N ^{161}Yb, the $\pi h_{11/2}[523]7/2^- \otimes \nu i_{13/2}[651]3/2^+$ configuration, i.e., $AA_p(B_p)$ with $K = 5$, is favored for band A. The levels in this band are assigned odd parity.

In Fig. 8, Routhians for the $\pi h_{11/2}$ bands in odd-A ^{161,163}Lu nuclei [20,21] and for the yrast $\pi h_{11/2} \otimes \nu i_{13/2}$ bands in the odd-odd ^{164}Lu nuclei [16,17] are also plotted. It is interesting to note that the energy signature splitting before the band crossing as observed in the yrast $\pi h_{11/2}$ bands in odd-A Lu isotopes is considerably reduced in the corresponding odd-odd isotopes. Similar behavior has also been observed in Ho [4–7,23] and Tm [9–14,24] isotopes. The large energy signature splitting in $\pi h_{11/2}$ bands in odd-A

TABLE I. Gamma transition energies, placements, intensities (I_γ), DCO ratios, branching ratios (λ), and $B(M1)/B(E2)$ ratios in ^{162}Lu.

E_γ (keV)[a]	Placement ($I_i \rightarrow I_f$)	I_γ (%)	DCO ratio	λ[b]	$\frac{B(M1,I_i \rightarrow I_i-1)}{B(E2,I_i \rightarrow I_i-2)}$ [c]
Band *A*					
108.3	below (10^-)	127(13)	1.16(18)		
161.0	below (10^-)	93(15)			
164.2	below (10^-)	151(15)	0.92(15)		
266.0	below (10^-)	278(42)			
268.3	below (10^-)	230(35)			
281.8	below (10^-)	198(31)			
143.6	(10^-)→(9^-)	214(17)	0.76(11)		
80.6	(11^-)→10^-)	159(16)	0.81(13)	0.65(11)	1.17(19)
224.7	(11^-)→(9^-)	103(12)	0.95(15)		
195.5	(12^-)→(11^-)	1349(130)	0.72(8)	0.224(31)	0.67(9)
276.2	(12^-)→(10^-)	302(30)	d		
160.5	(13^-)→(12^-)	1000(60)	0.72(8)	0.83(9)	1.15(13)
355.9	(13^-)→(11^-)	833(72)			
276.7	(14^-)→(13^-)	1413(98)	0.70(8)[d]	0.314(34)	1.66(18)
436.9	(14^-)→(12^-)	444(40)	0.89(12)		
234.2	(15^-)→(14^-)	937(72)	0.70(8)	1.34(13)	1.40(14)
510.5	(15^-)→(13^-)	1254(75)	1.05(8)		
326.1	(16^-)→(15^-)	897(62)	0.65(7)	0.69(8)	1.60(18)
560.0	(16^-)→(14^-)	619(50)	0.96(11)		
299.8	(17^-)→(16^-)	413(28)	0.54(7)	2.04(22)	1.21(13)
625.5	(17^-)→(15^-)	841(65)	0.98(10)		
356.6	(18^-)→(17^-)	452(41)	0.68(9)	1.09(14)	1.70(22)
656.1	(18^-)→(16^-)	492(46)	1.25(17)		
352.1	(19^-)→(18^-)	254(25)		2.44(34)	1.16(16)
708.7	(19^-)→(17^-)	619(62)	0.98(12)		
374.2	(20^-)→(19^-)	421(50)[d]	0.60(10)[d]	>1.09(17)	<2.4(4)
725.9	(20^-)→(18^-)	460(46)	0.99(15)		
382.5	(21^-)→(20^-)	198(28)	0.64(11)	1.80(32)	1.70(31)
756.1	(21^-)→(19^-)	357(40)	1.05(16)		
364.0	(22^-)→(21^-)	270(32)	0.67(12)	2.03(36)	1.63(29)
745.8	(22^-)→(20^-)	548(70)	1.10(18)[d]		
373.8	(23^-)→(22^-)	d	d		
737.8	(23^-)→(21^-)	262(31)			
339.6	(24^-)→(23^-)	214(29)	0.54(12)	1.8(4)	1.8(4)
713.9	(24^-)→(22^-)	381(57)			
370.9	(25^-)→(24^-)	230(35)		1.2(3)	2.0(5)
711.0	(25^-)→(23^-)	276(45)			
347.6	(26^-)→(25^-)	222(40)	0.52(14)	1.25(29)	2.5(6)
718.5	(26^-)→(24^-)	278(42)			
397.3	(27^-)→(26^-)	159(32)	0.63(15)	1.4(4)	1.8(5)
745.0	(27^-)→(25^-)	222(40)	d		
371	(28^-)→(27^-)	115(25)		1.5(5)	2.5(9)
768	(28^-)→(26^-)	168(40)			
434.7	feeding (28^-)	175(44)			
831.7	feeding (28^-)	218(52)			
Band *B*					
582.4	below (16^+)	850(120)	0.85(18)		
787.6	below (17^+)	296(45)	0.50(10)		
206.1	(17^+)→(16^+)	388(45)	0.55(10)		
192.7	(18^+)→(17^+)	646(52)	0.57(7)	0.49(8)	2.0(3)
398.3	(18^+)→(16^+)	320(45)			
195.8	(19^+)→(18^+)	845(90)	0.67(8)	0.61(9)	1.34(20)

TABLE I. (*Continued*.)

E_γ (keV)[a]	Placement $(I_i \rightarrow I_f)$	I_γ (%)	DCO ratio	λ[b]	$\frac{B(M1,I_i \rightarrow I_i-1)}{B(E2,I_i \rightarrow I_i-2)}$ [c]
388.8	$(19^+) \rightarrow (17^+)$	513(51)			
231.0	$(20^+) \rightarrow (19^+)$	893(71)	0.64(7)	0.44(6)	1.81(25)
427.0	$(20^+) \rightarrow (18^+)$	389(43)	1.02(14)		
260.6	$(21^+) \rightarrow (20^+)$	694(56)	0.66(7)	0.66(8)	1.70(20)
491.2	$(21^+) \rightarrow (19^+)$	456(40)	0.89(12)		
282.8	$(22^+) \rightarrow (21^+)$	693(55)	0.60(8)	0.58(7)	2.5(3)
542.6	$(22^+) \rightarrow (20^+)$	399(35)	1.05(14)		
317.8	$(23^+) \rightarrow (22^+)$	513(41)	0.60(8)	1.26(18)	1.33(19)
600.2	$(23^+) \rightarrow (21^+)$	646(78)			
338.7	$(24^+) \rightarrow (23^+)$	399(48)	0.62(9)	1.19(19)	1.81(29)
655.8	$(24^+) \rightarrow (22^+)$	475(52)	1.27(20)		
364.9	$(25^+) \rightarrow (24^+)$	256(31)	0.50(10)	1.48(27)	1.66(30)
703.1	$(25^+) \rightarrow (23^+)$	380(53)	0.95(18)		
395.8	$(26^+) \rightarrow (25^+)$	237(43)		1.12(26)	2.5(6)
760.8	$(26^+) \rightarrow (24^+)$	266(40)	1.16(26)		
402.9	$(27^+) \rightarrow (26^+)$	152(27)		1.9(5)	1.8(5)
798.7	$(27^+) \rightarrow (25^+)$	294(52)			
440.9	$(28^+) \rightarrow (27^+)$	256(60)[d]		$>1.0(3)$	$<3.3(11)$
844.0	$(28^+) \rightarrow (26^+)$	266(58)			
442	$(29^+) \rightarrow (28^+)$	d			
882.8	$(29^+) \rightarrow (27^+)$	180(45)			
Band *C*					
185.0	$X+1 \rightarrow X$	108(12)	0.48(10)		
210.3	$X+2 \rightarrow X+1$	228(23)	0.66(8)	0.36(5)	2.02(30)
395.3	$X+2 \rightarrow X$	81(9)	1.00(16)		
257.1	$X+3 \rightarrow X+2$	294(24)	0.64(6)	0.38(6)	2.4(4)
466.8	$X+3 \rightarrow X+1$	111(14)	1.04(18)		
246.3	$X+4 \rightarrow X+3$	282(20)	0.71(8)	0.67(10)	2.22(33)
502.8	$X+4 \rightarrow X+2$	189(24)	0.96(17)		
320.6	$X+5 \rightarrow X+4$	276(22)	0.67(8)	0.55(8)	2.21(33)
566.5	$X+5 \rightarrow X+3$	153(20)	1.00(18)		
294.3	$X+6 \rightarrow X+5$	204(16)	0.72(10)	1.03(14)	2.31(32)
614.5	$X+6 \rightarrow X+4$	210(24)	0.94(20)		
373.4	$X+7 \rightarrow X+6$	162(16)	0.73(10)	0.70(11)	2.5(4)
667.3	$X+7 \rightarrow X+5$	114(12)	1.04(20)		
358.2	$X+8 \rightarrow X+7$	105(13)	0.56(10)	1.40(24)	2.2(4)
730.8	$X+8 \rightarrow X+6$	147(18)	0.96(22)		
407.5	$X+9 \rightarrow X+8$	78(12)	0.49(10)[d]	1.42(26)	1.90(34)
765.7	$X+9 \rightarrow X+7$	111(15)	1.14(25)		
407.5	$X+10 \rightarrow X+9$	54(8)	d	2.0(5)	1.8(4)
815	$X+10 \rightarrow X+8$	108(20)			
434.4	$X+11 \rightarrow X+10$	90(18)		1.0(3)	3.6(10)
842.5	$X+11 \rightarrow X+9$	90(20)	1.3(5)		
454.4	$X+12 \rightarrow X+11$	39(12)		1.2(4)	3.4(15)
889.4	$X+12 \rightarrow X+10$	48(15)			

[a]Energies are accurate to 0.3 keV for strong transitions, increasing to about 0.8 keV for weaker transitions.
[b]Branching ratios λ, measured from spectra corresponding to gates above spin I. For higher spin states, λ were also deduced from spectra gated on low spin transitions.
[c]Assuming $\delta = 0$. For the errors only the uncertainties in λ have been taken into account.
[d]DCO ratio values determined for the doublets present within the same band.

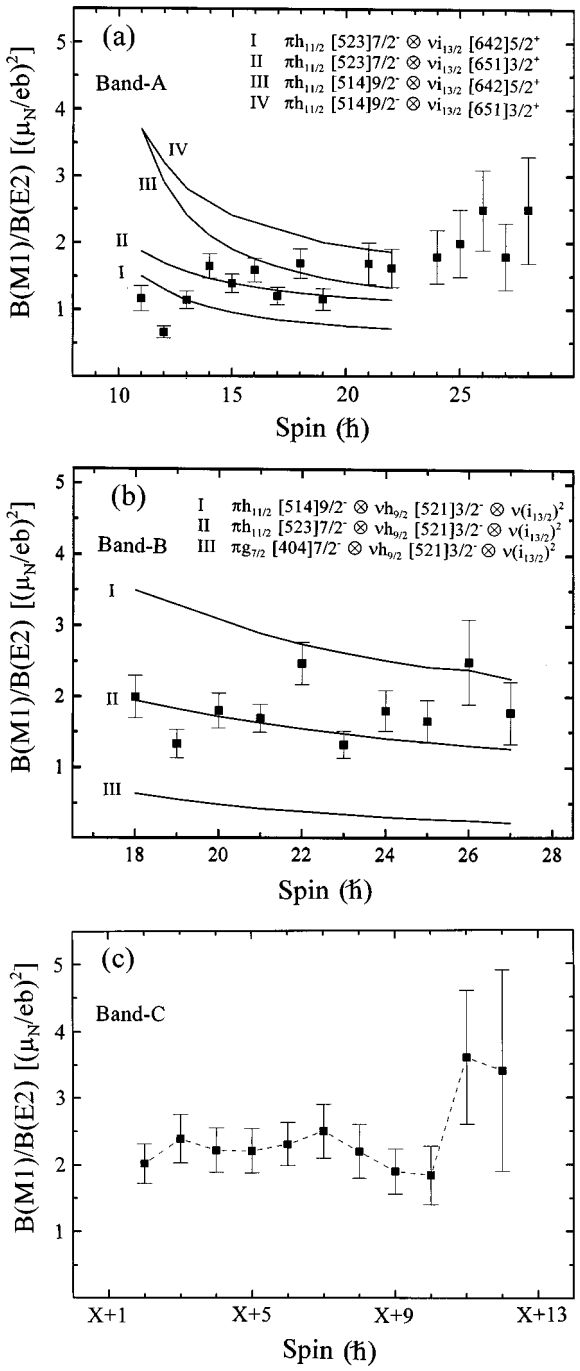

FIG. 5. Experimental $B(M1)/B(E2)$ ratios as a function of spin for (a) band A, (b) band B, and (c) band C in ^{162}Lu. The solid curves correspond to calculations based on geometric model of Donau and Frauendorf [46].

isotopes has been understood in terms of a sizable negative γ deformation [20–24]. On the other hand, in ^{162,164}Lu nuclei, since the odd neutron lies in the low Ω $(=3/2,5/2)$ $i_{13/2}$ orbitals, it influences the polarization of the nuclear core more than the odd proton, resulting in a net small positive γ deformation [57]. The self-consistent calculations of total Routhian surfaces (TRS's) [58–60] performed for the yrast band configuration in ^{162}Lu predict $\beta_2 \approx 0.19$ and a small positive γ deformation ($\gamma \sim 2°$) up to $\hbar\omega = 0.45$ MeV, in line with the inference drawn above.

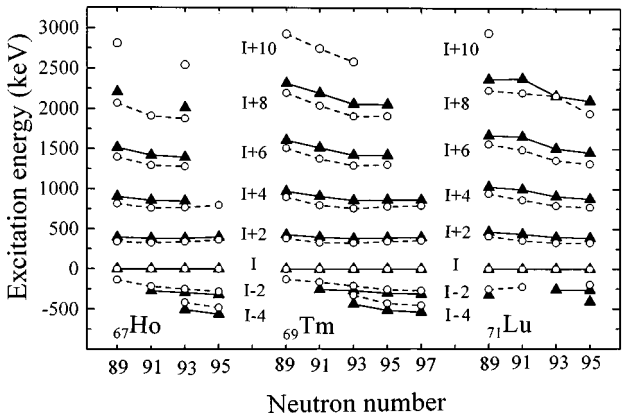

FIG. 6. Level energy systematics of the $\pi h_{11/2} \otimes \nu i_{13/2}$ bands in odd-odd $^{156-162}$Ho [3–8,48], $^{158-166}$Tm [9–14], and ^{160,164,166}Lu [15–18,48]. The levels at $I=11$ and 12 are used as reference energy for the $\alpha=1$ signature (open circle) and $\alpha=0$ signature (solid triangle), respectively. The level energies of yrast band in ^{162}Lu (present work) fit well in the systematics.

B. Band *B*

Band B (Fig. 3) decays via strong 787.6 keV [from the (17^+) level] and 582.4 keV [from the (16^+) level] transitions as seen in the gated coincidence spectrum [Fig. 4(d)]. The observation of a 787.6 keV crossover transition and the 206.1 keV $[(17^+)\rightarrow(16^+)]$ and 582.4 keV stopover transitions do indicate that a common level (possibly isomeric) is populated in their decay. However, the measured DCO ratios for the 582.4 and 787.6 keV transitions (Table I) indicate these to be mainly quadrupole and dipole, respectively, and hence these transitions do not form a part of the coupled rotational structure of this band. Band B at spin (17^+) also feeds to the levels of band A at and below $I^\pi=(16^-)$ with an intensity of $\sim$20%. Assuming the 600 keV linking transition to be dipole, the spin to the lowest shown level in band B has been tentatively assigned as $I=16\hbar$.

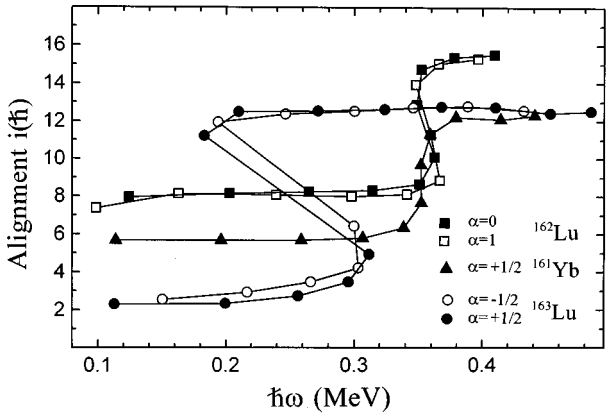

FIG. 7. (a) Measured alignments for (i) the $\pi h_{11/2}[523]7/2^- \otimes \nu i_{13/2}[651]3/2^+$ band (band A) in ^{162}Lu, (ii) the $\pi h_{11/2}[523]7/2^-$ band in ^{163}Lu [21,49], and (iii) the $\nu i_{13/2}[651]3/2^+$ band in ^{161}Yb [42]. $J_0=22$ MeV^{-1} $\hbar^2$, $J_1=58$ MeV^{-3} $\hbar^4$ [21], and $J_0=18$ MeV^{-1} $\hbar^2$, $J_1=90$ MeV^{-3} $\hbar^4$ [42] are used as reference core parameters in the case of ^{163}Lu and ^{161}Yb, ^{162}Lu nuclei, respectively.

TABLE II. The alignment values i_p and i_n at $\hbar\omega = 0.20$ MeV before the band crossing for different band configurations in ^{162}Lu and neighboring odd-A Yb and Lu nuclei.

Band	Nucleus[a]	Reference core parameters[a] J_0	J_1	Alignment[b] (i_n, i_p) at $\hbar\omega = 0.20$ MeV
$\nu i_{13/2}[651]3/2^+$	^{161}Yb [42]	18.0	90.0 [42]	5.7
$\pi h_{11/2}[514]9/2^-$	^{161}Lu [20][c]	16.0	90.0 [42]	3.2(2.7)
$\nu i_{13/2}[642]5/2^+$	^{163}Yb [44]	23.0	90.0 [44]	5.4
$\nu h_{9/2}[521]3/2^-$	^{163}Yb [44]	23.0	90.0 [44]	3.2
$\pi h_{11/2}[523]7/2^-$	^{163}Lu [21]	22.0	58.0 [21]	2.8(2.3)
$\pi g_{7/2}[404]7/2^+$	^{163}Lu [21]	22.0	58.0 [21]	0.8(0.8)
$\pi h_{11/2}[514]9/2^-$	^{165}Lu [22]	25.8	90.0 [33]	2.4(2.2)
$\pi h_{9/2}[541]1/2^-$	^{165}Lu [22]	25.8	90.0 [33]	3.4
$\pi g_{7/2}[404]7/2^+$	^{165}Lu [22]	25.8	90.0 [33]	0.8
$\pi d_{5/2}[402]5/2^+$	^{165}Lu [22]	25.8	90.0 [33]	0.3(0.1)
$\pi d_{3/2}[411]1/2^+$	^{165}Lu [22]	25.8	90.0 [33]	0.6(0.4)
$\pi h_{11/2}[514]9/2^- \otimes$	^{162}Lu	18.0	90.0 [42]	7.7
$\nu i_{13/2}[642]5/2^+$				7.8[d]
$\pi h_{11/2}[523]7/2^- \otimes$	^{162}Lu	18.0	90.0 [42]	7.9
$\nu i_{13/2}[642]5/2^+$				8.2[d]
$\pi h_{11/2}[514]9/2^- \otimes$	^{162}Lu	18.0	90.0 [42]	7.9
$\nu i_{13/2}[651]3/2^+$				8.1[d]
$\pi h_{11/2}[523]7/2^- \otimes$	^{162}Lu	18.0	90.0 [42]	8.1
$\nu i_{13/2}[651]3/2^+$				8.5[d]

[a]Numbers within the square brackets indicate references.
[b]Alignment values within paranthesis correspond to the unfavored signature partner.
[c]Configuration tentatively assigned, other possibility is $\pi h_{11/2}[523]7/2^-$.
[d]$(i_n + i_p)$ value.

The large initial alignment of $\sim 14\hbar$ observed for this band (Fig. 9) is indicative of a four-quasiparticle structure involving the coupling of the odd neutron and the odd proton with a pair of aligned quasiparticles ($i_{13/2}$ quasineutrons).

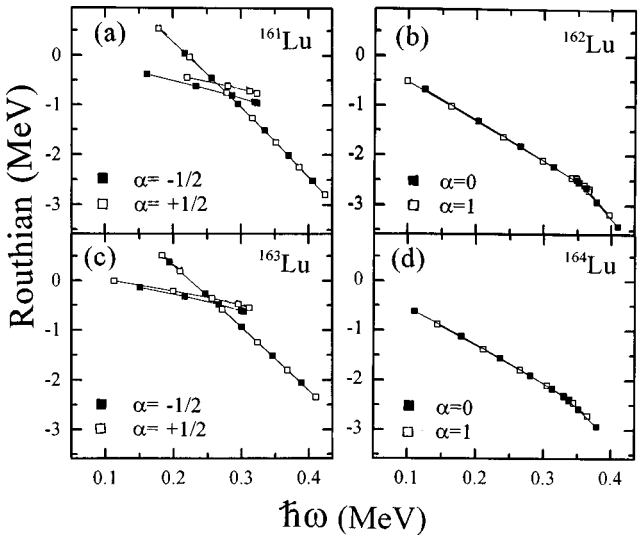

FIG. 8. Experimental Routhians corresponding to the $\pi h_{11/2} \otimes \nu i_{13/2}$ bands in ^{162}Lu (present work) and ^{164}Lu [16,17], and the $\pi h_{11/2}$ bands in ^{161,163}Lu [20,21].

TABLE III. Systematics of the $A \rightarrow ABC$ crossing frequencies for ^{162}Lu and neighboring odd-N even-Z and odd-odd nuclei.

Nucleus	Crossing frequency (MeV)
^{161}Yb	0.35 [41]
^{163}Yb	0.36 [44]
^{165}Yb	0.36 [50]
^{163}Hf	0.36 [51]
^{165}Hf	0.34 [51]
^{162}Tm	$\sim$0.35 [11,12]
^{162}Lu	0.35 [present work]
^{164}Lu	$\sim$0.35 [16,17]
^{166}Lu	$\sim$0.32 [18]

The part of the band before quasiparticle pair alignment is not being observed. Since this band feeds to band A at low excitation energy (or low frequencies), it is most likely that the unobserved part of band B involves alignment of an $i_{13/2}$ neutron pair (AB crossing), which is expected to occur at the lowest crossing frequency and have a large alignment gain of $\sim 9\hbar$ [33]. The possibility of BC ($\nu i_{13/2}$ pair) or A_pB_p ($\pi h_{11/2}$ pair) band crossing in the unobserved part of band B is very unlikely as these are expected to have a lesser alignment gain of (4–6)$\hbar$ and occur at higher frequencies (>0.32 MeV) [20,33]. Also, no BC band crossing is seen in the observed part of the band (Fig. 9). In view of the above, the odd neutron in the configuration of band B is not the $i_{13/2}$ neutron. The likely orbital for the odd neutron could be $\nu h_{9/2}[521]3/2^-$ (E orbital), which is close to the Fermi surface. Also, $\nu h_{9/2}[521]3/2^-$ is one of the favored configurations in the neighboring odd-N ^{161,163}Yb nuclei [42,44]. Negligibly small signature splitting ($\Delta e' \leqslant 5$ keV) is observed in this band.

The experimental $B(M1)/B(E2)$ values deduced from this band are compared, in Fig. 5(b), with the values calcu-

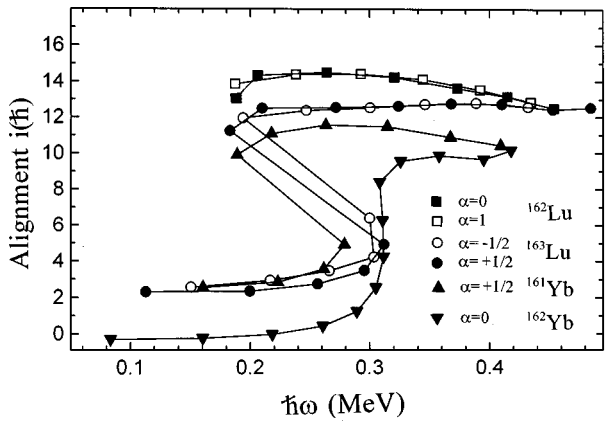

FIG. 9. Measured alignments for (i) the $\pi h_{11/2}[523]7/2^- \otimes \nu h_{9/2}[521]3/2^- \otimes (\nu i_{13/2})^2$ band (band B) in ^{162}Lu, (ii) the $\pi h_{11/2}[523]7/2^-$ band in ^{163}Lu [21,49], (iii) the ground state band in ^{162}Yb [42,43], and (iv) the $\nu i_{13/2}[521]3/2^-$ band in ^{161}Yb [42]. ($J_0 = 22$ MeV^{-1} $\hbar^2$, $J_1 = 58$ MeV$^{-3}\hbar^4$ [21]), ($J_0 = 20$ MeV^{-1} $\hbar^2$, $J_1 = 90$ MeV^{-3} $\hbar^4$ [21]), and ($J_0 = 18$ MeV^{-1} $\hbar^2$, $J_1 = 90$ MeV^{-3} $\hbar^4$ [42]) are used as reference core parameters in the case of ^{163}Lu, ^{162}Yb, and ^{162}Lu, ^{161}Yb nuclei, respectively.

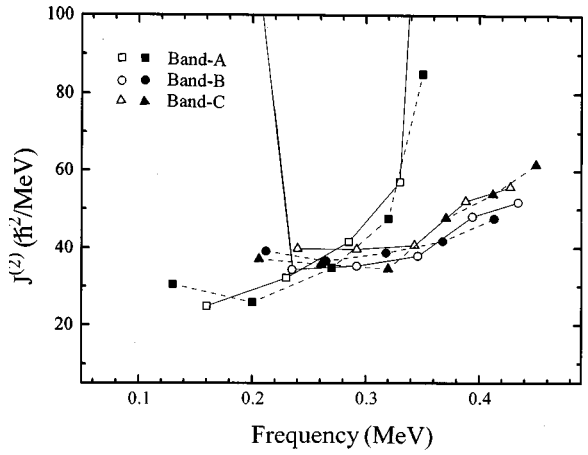

FIG. 10. Plot of dynamic moment of inertia $[J^{(2)}]$ for the bands A, B, and C in ^{162}Lu.

lated using Eqs. (2)–(4) for the $\pi h_{11/2}[523]7/2^-$ (or $\pi h_{11/2}[514]9/2^-)\otimes\nu h_{9/2}[521]3/2^-$ and $\pi g_{7/2}[404]7/2^+ \otimes \nu h_{9/2}[521]3/2^-$ configurations after the alignment of the $\nu i_{13/2}$ pair. The parameters used for the theoretical calculations are $g_p=1.32$ [21], $i_p=2.4\hbar$ for $\pi h_{11/2}[514]9/2^-$, $g_p=1.41$ [53], $i_p=2.8\hbar$ for $\pi h_{11/2}[523]7/2^-$, $g_p=0.62$ [21], $i_p=0.8\hbar$ for $\pi g_{7/2}[404]7/2^+$, $g_n=0.22$ [61], $i_n=3.2\hbar$ for the $\nu h_{9/2}[521]3/2^-$, and $g_n=-0.22$ [52], $i_n=9.3\hbar$ [33] for the aligned $(\nu i_{13/2})^2$ quasiparticles. It is clear from Fig. 5(b) that the calculated $B(M1)/B(E2)$ values for the $\pi h_{11/2}[523]7/2^-\otimes\nu h_{9/2}[521]3/2^-\otimes(\nu i_{13/2})^2$ configuration agree well with the measured ones. The observed alignment $\sim 14\hbar$ for this band is fairly reproduced by adding the alignment contributions of $2.8\hbar$ from $\pi h_{11/2}[523]7/2^-$ [21], $3.2\hbar$ from $\nu h_{9/2}[521]3/2^-$ [42], and $9.3\hbar$ from the aligned $(\nu i_{13/2})^2$ quasiparticles [33] (Fig. 9). Therefore, the $\pi h_{11/2}[523]7/2^-\otimes\nu h_{9/2}[521]3/2^-\otimes(\nu i_{13/2})^2$, i.e., $EABA_p(B_p)$, configuration is assigned for band B. The levels in this band are assigned even parity.

C. Band *C*

The coupled band C (Fig. 3) is not found to have links with either of bands A or B. A number of gamma peaks, labeled (▼) in Figs. 4(e) and 4(f), are seen consistently in the gated coincidence spectra of transitions of this band. These transitions could not be placed in the level scheme due to possible contaminations from other sequences/reaction channels and low statistics. It is likely that these transitions occur in the lower part of the band. This band has more or less constant alignment, signature splitting ~ 20 keV, and large $B(M1)/B(E2)$ values ~ 2.2 [Fig. 5(c)]. The small signature splitting and higher $B(M1)/B(E2)$ values are similar to those found in band B, suggesting that the signature-active particle in band C is also an $h_{11/2}$ proton. In Fig. 10, dynamic moment of inertia $(J^{(2)})$ for band C is compared with that for bands A and B. For band A, $J^{(2)}$ shows a sharp increase around 0.32 MeV because of the occurrence of BC band crossing. For bands B and C, $J^{(2)}$ is fairly constant over the frequency range $\sim 0.20-0.35$ MeV for both the signatures and afterwards shows a small increasing trend. In view of the above-mentioned similarities with band B, it is likely that band C is also a four-quasiparticle band, where AB neutron

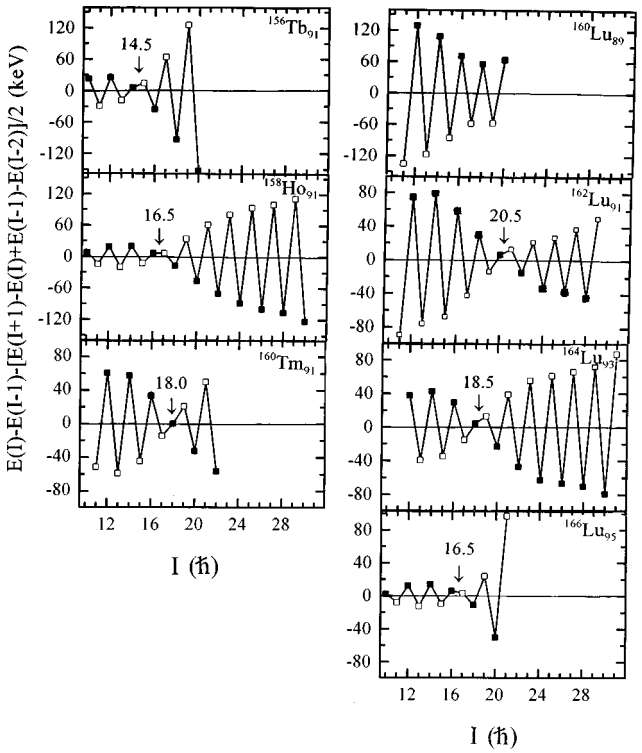

FIG. 11. $S=E(I)-E(I-1)-[(E(I+1)-E(I)+E(I-1)-E(I-2)]/2$ as a function of spin (I) for the $\pi h_{11/2}\otimes\nu i_{13/2}$ yrast band in ^{162}Lu (present work) along with that in the ^{160,164,166}Lu isotopes [15–18], and the ^{156}Tb [2], ^{158}Ho [5,6], and ^{160}Tm [10] $(N=91)$ isotones. Solid and open symbols correspond to the favored and unfavored signature partners, respectively. The spin at which signature inversion occurs is indicated by a vertical arrow.

alignment has already taken place in the unobserved part of the band. The configuration assigned to band C is, therefore, $FABA_p(B_p)$, similar to $EABA_p(B_p)$ of band B. Such quasineutron structures $EAB(FAB)$ have been observed in the neighboring odd-N ^{161,163}Yb nuclei [42,44]. The participation of unfavored quasineutron F in the configuration of band C is also supported by the weaker intensity flow through this band than in band B.

D. Anomalous signature splitting and signature inversion in band *A*

The experimental Routhians of the favored signature $\alpha_f=0$ (even spins) of the $\pi h_{11/2}\otimes\nu i_{13/2}$ yrast band in ^{162}Lu [Fig. 8(b)] are found to lie higher in energy as compared to that of the unfavored signature $\alpha_u=1$ (odd spins), at lower rotational frequencies (anomalous signature splitting). As the rotational frequency is increased, the two Routhians cross (signature inversion) at a frequency $\hbar\omega_c=0.37$ MeV and signature dependence becomes normal. This is not evident from Fig. 8(b) due to small signature splitting. This phenomenon of signature inversion has also been observed in various odd-odd rare-earth nuclei like ^{152}Eu [1], ^{154,156}Tb [2], $^{156-162}$Ho [3–8], $^{160-166}$Tm [10–14], ^{164,166}Lu [16–18], and ^{168}Ta [19]. To illustrate the systematics of this phenomenon, a more sensitive term $S=E(I)-E(I-1)-[E(I+1)-E(I)+E(I-1)-E(I-2)]/2$ has been plotted in Fig. 11 as a function of spin (I) for the odd-odd ^{162}Lu along with the ^{160,164,166}Lu [15–18,48] isotopes and the ^{156}Tb [2,48],

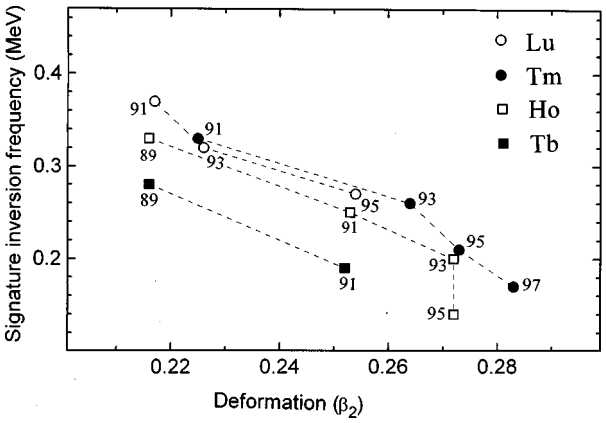

FIG. 12. Systematics of signature inversion frequency for the $\pi h_{11/2} \otimes \nu i_{13/2}$ yrast bands in the odd-odd ^{154,156}Tb [2,48], $^{156-162}$Ho [3–8,48], $^{160-166}$Tm [10–14], ^{162}Lu (present work), ^{164,166}Lu [16–18,48], and ^{168}Ta [19,48] nuclei as a function of ground state deformation (β_2) [62]. Each point is labeled with the neutron number of the corresponding nucleus.

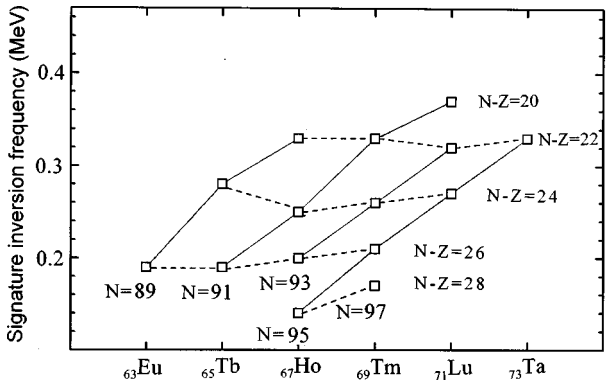

FIG. 13. Systematics of signature inversion frequency for the $\pi h_{11/2} \otimes \nu i_{13/2}$ yrast bands in the odd-odd ^{152}Eu [1], ^{154,156}Tb [2,48], $^{156-162}$Ho [3–8,48], $^{160-166}$Tm [10–14], ^{162}Lu (present work), ^{164,166}Lu [16–18,48] and ^{168}Ta [19,48] nuclei. Solid lines correspond to nuclei with same N and dotted lines correspond to nuclei with same $N-Z$, as labeled in the figure.

^{158}Ho [4,5,48], and ^{160}Tm [10] ($N=91$) isotones. It is clear from this figure that the staggering magnitude of signature dependence below the inversion point decreases with increasing N in the Lu isotopes and increases with increasing Z in the $N=91$ isotones. Similar behavior has also been observed for the ^{154,156}Tb [2,48], $^{156-162}$Ho [3–8,48], and $^{160-166}$Tm [9–13] isotopes. The inversion point shifts to lower spins with increasing N in Lu isotopes and to higher spins with increasing Z in $N=91$ isotones. The rotational frequency at which signature inversion occurs has also been plotted, as a function of ground state quadrupole deformation (β_2) [62] in Fig. 12, for ^{154,156}Tb, $^{156-162}$Ho, $^{160-166}$Tm, and $^{162-166}$Lu isotopes. For different chains of isotopes, the signature inversion frequency decreases with increase in β_2. This deformation-dependent behavior of signature inversion was also pointed out by us earlier [16]. An additional $(N-Z)$ effect on the signature inversion frequencies is seen in Fig. 13. Interestingly, for $(N-Z)=22$, 24, 26, and 28, the signature inversion frequency remains practically unchanged.

A number of theoretical attempts [25–32] have been made to understand the phenomenon of signature inversion in the $\pi h_{11/2} \otimes \nu i_{13/2}$ bands of rare-earth odd-odd nuclei, as have been summarized by us earlier [16]. Since the signature inversion frequency varies over a large frequency range (0.14–0.37 MeV), over which nuclear behavior changes in a complex manner, any one explanation for the signature inversion phenomenon is probably insufficient. In order to establish a reliable understanding of the observed trends, more comprehensive calculations are needed.

In conclusion, our work establishes for the first time high spin band structure involving three signature-split bands in the odd-odd nucleus ^{162}Lu. Nilsson configurations have been assigned to these bands. In the $\pi h_{11/2} \otimes \nu i_{13/2}$ yrast band, both signature partners show an upbend at a rotational frequency $\hbar\omega = 0.35$ MeV, indicating the occurrence of two-$i_{13/2}$-quasi neutron BC crossing. In the same band, anomalous signature splitting has been observed with signature inversion at $I \sim 20\hbar$. Band B is found to feed levels of band A below $I = 16\hbar$ and exhibits large initial alignment. It has been assigned a four-quasiparticle configuration $\pi h_{11/2}[523]7/2^- \otimes \nu h_{9/2}[521]3/2^- \otimes (\nu i_{13/2})^2$, i.e., $EABA_p(B_p)$. Band C, which is not found to have links with either band A or B, shows similar behavior in moment of inertia, alignment, and $B(M1)/B(E2)$ values as those found in band B. It is probably a band based on a similar four-quasiparticle configuration involving an F quasineutron, i.e., $FABA_p(B_p)$.

ACKNOWLEDGMENTS

The authors are grateful to Herbert Hübel and W. Korten for their useful suggestions and comments. Thanks are also due to the Pelletron accelerator staff of the Nuclear Science Centre, New Delhi, for their excellent support during the experiment. This work was carried out under research project No. UFUP-P3 funded by University Grants Commission, New Delhi.

[1] J. A. Pinston, R. Bengtsson, E. Monnand, F. Schussler, and D. Barneoud, Nucl. Phys. **A361**, 464 (1981).

[2] R. Bengtsson, J. A. Pinston, D. Barneoud, E. Monnand, and F. Schussler, Nucl. Phys. **A389**, 158 (1982).

[3] S. H. Bhatti, J. C. Kim, S. J. Chae, J. H. Ha, C. S. Lee, J. Y. Moon, C. B. Moon, T. Kamatsubara, J. Lu, M. Matsuda, T. Hayakawa, T. Watanabe, and K. Furuno, Z. Phys. A **353**, 119 (1995).

[4] D. M. Cullen, C.-H. Yu, D. Cline, M. Simon, and D. C. Radford, Nuclear Structure Research Laboratory, University of Rochester, Annual Report, 1994, p. 22.

[5] N. Rizk and J. Bontel, J. Phys. (France) Lett. **37**, L197 (1976).

[6] C.-H. Yu, D. M. Cullen, D. Cline, M. Simon, D. C. Radford, I. Lee, and A. O. Macchiavelli, Nuclear Structure Research Lab, University of Rochester, Annual Report 1994, p. 28.
[7] S. Drissi, Z. Li, M. Délèze, J. Kern, and J. P. Vorlet, Nucl. Phys. **A600**, 63 (1996).
[8] R. G. Helmer, Nucl. Data Sheets **64**, 79 (1991).
[9] M. A. Riley, Y. A. Akovali, C. Baktash, M. L. Halbert, D. C. Hensley, N. R. Johnson, I. Y. Lee, F. K. McGowan, A. Virtanen, L. H. Courtney, V. P. Janzen, L. L. Riedinger, L. Chaturvedi, and J. Simpson, Phys. Rev. C **39**, 291 (1989); S. Andre, D. Barnéoud, C. Foin, J. Genevey, and J. C. Merdinger, Z. Phys. A **332**, 233 (1989).
[10] S. Andre, D. Barnéoud, C. Foin, J. Genevey, J. A. Pinston, B. Haas, J. P. Vivien, and A. J. Kreiner, Z. Phys. A **333**, 247 (1989).
[11] J. M. Espino, C. Martinez-Torre, G. B. Hagemann, H. J. Jensen, P. O. Tjom, A. Atac', M Bergstrom, A. Bracco, A. Brockstedt, H. Carlsson, L. P. Ekström, B. Herskind, F. Ingebretsen, J. Jongman, S. Leoni, R. M. Lieder, T. Lönroth, A. Maj, B. Million, A. Nordlund, J. Nyberg, M. Piiparinen, H. Ryde, M. Sugawara, and A. Virtanen, The Niels Bohr and NORDITA Research Activity Report, 1995, p. 99.
[12] S. Drissi, J. Cl. Dousse, V. Ionescu, J. Kern, J. A. Pinston, and D. Bernéoud, Nucl. Phys. **A466**, 385 (1987).
[13] X. Z. Wang, W. Reviol, L. L. Riedinger, H. J. Jensen, G. B. Hagemann, P. O. Tjom, R. A. Bark, S. Leoni, T. Lönnroth, H. Schnack-Petersen, T. Shizuma, J. Wrzesinski, and J.-Y. Zhang, The Niels Bohr and NORDITA Research Activity Report, 1995, p. 102.
[14] S. Drissi, A. Bruder, M. Carlen, J. Vl. Dousse, M. Gasser, J. Kern, S. J. Mannamal, B. Perny, Ch. Rheme, J. L. Salicio, J. P. Vorlet, and I. Hamamoto, Nucl. Phys. **A543**, 495 (1992).
[15] H. Sun, Y. Ma, J. Zhang, H. Zheng, S. Zhou, Y. Liu, S. Wen, G. Li, G. Yuan, and C. Yang, Z. Phys. A **352**, 115 (1995).
[16] P. Juneja, S. L. Gupta, S. C. Pancholi, A. Kumar, D. Mehta, L. Chaturvedi, S. K. Katoch, S. Malik, G. Shanker, R. K. Bhowmik, S. Muralithar, G. Rodrigues, and R. P. Singh, Phys. Rev. C **53**, 1221 (1996).
[17] X.-H. Wang, C.-H. Yu, D. M. Cullen, D. C. Bryan, M. Devlin, M. J. Fitch, A. Galindo-Uribarri, R. W. Gray, D. M. Herrick, R. W. Ibbotson, K. L. Kurz, S. Mullins, S. Pilotte, D. C. Radford, M. R. Satteson, M. W. Simon, D. Ward, C. Y. Wu, and L. H. Yao, Nucl. Phys. **A608**, 77 (1996).
[18] D. Hojman, A. J. Kreiner, M. Davidson, J. Davidson, M. Debray, E. W. Cybulska, P. Pascholati, and W. A. Seale, Phys. Rev. C **45**, 90 (1992).
[19] K. Theine, C.-X. Yang, A. P. Byrne, H. Hübel, R. Chapman, D. Clarke, F. Khazaie, J. C. Lisle, J. N. Mo, J. D. Garrett, and H. Ryde, Nucl. Phys. **A536**, 419 (1992).
[20] C.-H. Yu, M. A. Riley, J. D. Garrett, G. B. Hagemann, J. Simpson, P. D. Forsyth, A. R. Mokhtar, J. D. Morrison, B. M. Nyako, J. F. Sharpey-Schafer, and R. Wyss, Nucl. Phys. **A489**, 477 (1988).
[21] W. Schmitz, C.-X. Yang, H. Hübel, A. P. Byrne, R. Musseler, N. Singh, K. H. Maier, A. Kuhnert, and R. Wyss, Nucl. Phys. **A539**, 112 (1992).
[22] P. Frandsen, R. Chapman, J. D. Garrett, G. B. Hagemann, B. Herskind, C.-H. Yu, K. Schiffer, D. Clarke, F. Khazaie, J. C. Lisle, J. N. Mo, L. Carlen, P. Ekström, and H. Ryde, Nucl. Phys. **A489**, 508 (1988).
[23] D. C. Radford, H. R. Andrews, G. C. Ball, D. Horn, D. Ward, F. Banville, S. Flibotte, S. Monaro, S. Pilotte, P. Taras, J. K. Johansson, D. Tucker, J. C. Waddington, M. A. Riley, G. B. Hagemann, and I. Hamamoto, Nucl. Phys. **A545**, 665 (1992).
[24] S. J. Warburton, R. Chapman, J. Copnell, F. Liden, A. G. Smith, J. P. Sweeney, D. M. Thompson, S. J. Freeman, G. B. Hagemann, and M. Piiparinen, Nucl. Phys. **A591**, 323 (1995).
[25] R. Bengtsson, H. Frisk, F. R. May, and J. A. Pinston, Nucl. Phys. **A415**, 189 (1984).
[26] M. Matsuzaki, Phys. Lett. B **269**, 23 (1991).
[27] I. Hamamoto, Phys. Lett. B **235**, 221 (1990).
[28] P. Semmes and I. Ragnarrson, in *Proceedings of the International Conference on High Spin Physics and Gamma Soft Nuclei*, Pittsburgh, 1990, edited by J. X. Saladin, R. A. Sorensen, and C. M. Vincent (World Scientific, Singapore, 1991), p. 500.
[29] A. K. Jain and A. Goel, Phys. Lett. B **277**, 233 (1992).
[30] K. Hara and Y. Sun, Nucl. Phys. **A531**, 221 (1991).
[31] K. Hara, Nucl. Phys. **A557**, 449c (1993).
[32] N. Yoshida, H. Sagawa, and J. Otsuka, Nucl. Phys. **A567**, 17 (1994).
[33] S. Jönsson, N. Roy, H. Ryde, W. Waluś, J. Kownacki, J. D. Garrett, G. B. Hagemann, B. Herskind, R. Bengtsson, and S. Åberg, Nucl. Phys. **A449**, 537 (1986).
[34] P. Juneja *et al.*, DAE Symposium, Nucl. Phys. **B35**, 20 (1992); **B36**, 10 (1993); S. C. Pancholi, in *Proceedings of the International Workshop on Physics with Recoil Separators and Detector Arrays*, edited by R. K. Bhowmik and A. K. Sinha (Allied, New Delhi, 1995), p. 298
[35] S. G. Zhou, Y. Z. Liu, Y. J. Ma, and C. X. Yang, J. Phys. G **22**, 415 (1996).
[36] Y. H. Zhang, X. H. Zhou, O. Z. Zhao, X. F. Sun, X. G. Lei, Y. X. Guo, Z. Liu, X. F. Chen, S. X. Wen, G. J. Yuan, and X. A. Liu, Z. Phys. A **355**, 335 (1996).
[37] M. A. Cardona, M. E. Debray, D. Hojman, A. J. Kreiner, H. Somacal, J. Davidson, M. Davidson, D. De Acuña, J. Rico, D. Bazzacco, R. Borch, S. M. Lenzi, C. Rossi Alvarez, N. Blasi, and G. Lo Bianco, Z. Phys. A **354**, 5 (1996).
[38] A. Gavron, Phys. Rev. C **21**, 230 (1980).
[39] U. J. Schrewe, E. Hagberg, H. Schmeing, J. C. Hardy, V. T. Koslowsky, K. S. Sharma, and E. T. H. Vlifford, Phys. Rev. C **25**, 3091 (1982).
[40] H. J. Helmer, Nucl. Data Sheets **64**, 79 (1991).
[41] S. C. Pancholi and R. K. Bhowmik, Indian J. Pure Appl. Phys. **27**, 660 (1989).
[42] L. L. Riedinger, Nucl. Phys. **A347**, 141 (1980).
[43] J. N. Mo, S. Sergiwa, R. Chapman, J. C. Lisle, E. S. Paul, J. C. Willmott, J. Hattula, M. Jaakelainen, J. Simpson, P. M. Walker, J. D. Garrett, G. B. Hagemann, B. Herskind, M. A. Riley, and G. Sletten, Nucl. Phys. **A472**, 295 (1987).
[44] J. Kownacki, J. D. Garrett, J. J. Gaardhoje, G. B. Hagemann, B. Herskind, S. Jönsson, N. Roy, H. Ryde, and W. Waluś, Nucl. Phys. **A394**, 269 (1983).
[45] A. Kramer-Flecken, T. Morek, R. M. Lieder, W. Gast, G. Hebbinghaus, H. M. Jager, and W. Urban, Nucl. Instrum. Methods Phys. Res. A **275**, 333 (1989).
[46] F. Dönau and S. Frauendorf, in *Proceedings of the Conference on High Angular Momentum Properties of Nuclei*, Oak Ridge, Tennessee, 1982, edited by N. R. Johnson (Harwood Academic, Chur, Switzerland, 1982), p. 143.
[47] H. Behrens, Ph.D. thesis, Technical University, Munich, 1980.
[48] Y. Liu, Y. Ma, H. Yang, and S. Zhou, Phys. Rev. C **52**, 2514 (1995).

[49] W. Schmitz, H. Hübel, C. X. Yang, G. Baldsiefen, U. Birkental, G. Frohlingsdorf, D. Mehta, R. Mußler, M. Neffgen, J. Gascon, G. B. Hagemann, A. Maj, D. Muller, J. Nyberg, M. Piiparinen, A. Virtanen, and R. Wyss, Phys. Lett. B **303**, 230 (1993).
[50] N. Roy, S. Jönsson, H. Ryde, W. Waluś, J. J. Gaardhoje, J. D. Garrett, G. B. Hagemann, and B. Herskind, Nucl. Phys. **A382**, 125 (1981).
[51] K. P. Blume, H. Hübel, M. Murzel, J. Recht, K. Theine, H. Kluge, A. Kuhnert, K. H. Maier, A. Maj, M. Guttormsen, and A. P. De Lima, Nucl. Phys. **A464**, 445 (1987).
[52] H. Hübel, Fortschr. Phys. **25**, 327 (1977).
[53] R. A. Bark, G. D. Dracoulis, A. E. Stuchbery, A. P. Byrne, A. M. Baxter, F. Reiss, and P. K. Weng, Nucl. Phys. **A501**, 157 (1989).
[54] O. Prior, F. Boehm, and S. G. Nilsson, Nucl. Phys. **A110**, 257 (1968).
[55] C. J. Gallagher, Jr. and S. A. Moszkowski, Phys. Rev. **111**, 1282 (1958).
[56] M. P. Fewell, N. R. Jonsson, F. K. McGowan, J. S. Hatula, I. Y. Loe, C. Baktash, Y. Schutz, J. C. Wells, L. L. Riedinger, M. V. Guidri, and S. C. Pancholi, Phys. Rev. C **37**, 101 (1988).
[57] S. Frauendorf and F. R. May, Phys. Lett. **125B**, 245 (1983).
[58] W. Nazarewicz, G. A. Leander, and J. Dudek, Nucl. Phys. **A467**, 437 (1987).
[59] R. Wyss, J. Nyberg, A. Johnson, R. Bengtsson, and W. Nazarewicz, Phys. Lett. B **215**, 211 (1988).
[60] W. Nazarewicz, R. Wyss, and A. Johnson, Nucl. Phys. **A503**, 285 (1989).
[61] P. Raghvan, At. Data Nucl. Data Tables **42**, 189 (1989).
[62] P. Möller, J. R. Nix, W. D. Myers, and W. J. Swiatecki, At. Data Nucl. Data Tables **59**, 185 (1995).